

## ORIGINAL PAPER

# Digitized pathology: theory and experiences in automated tissue-based virtual diagnosis

K. KAYSER<sup>1)</sup>, D. RADZISZOWSKI<sup>2)</sup>, P. BZDYL<sup>2)</sup>,  
R. SOMMER<sup>3)</sup>, G. KAYSER<sup>4)</sup>

<sup>1)</sup>*UICC–TPCC, Charité, University of Berlin, Germany*

<sup>2)</sup>*AGH–UST Krakow, Poland*

<sup>3)</sup>*Cairo Consult, Mannheim, Germany*

<sup>4)</sup>*Institute of Pathology, University of Freiburg, Germany*

### Abstract

**Aims.** To describe the theory and develop an automated virtual slide screening system. *Theoretical considerations.* Tissue-based diagnosis separates into (a) sampling procedure to allocate the slide area containing diagnostic information, and (b) evaluation of diagnosis from the selected area. Nyquist's theorem broadly applied in acoustics, serves to presetting the sampling accuracy. Tissue-based diagnosis relies on two different information systems: (a) texture, and (b) object information. Texture information can be derived by recursive formulas without image segmentation. Object information requires image segmentation and feature extraction. Both algorithms complete another to a "self-learning" classification system. *Methods.* Non-overlapping compartments of the original virtual slide (image) are chosen at random with predefined error-rate (Nyquist's theorem). The standardized image compartments are subject for texture and object analysis. The recursive formula of texture analysis computes median gray values and local noise distribution. Object analysis includes automated measurements of immunohistochemically stained slides. The computations performed at different magnifications ( $\times 2$ ,  $\times 4.5$ ,  $\times 10$ ,  $\times 20$ ,  $\times 40$ ) are subject to multivariate statistically analysis and diagnosis classification. *Results.* A total of 808 lung cancer cases of diagnoses groups: cohort (1) normal lung (318 cases) – cancer (490 cases); cancer subdivided: cohort (2) small cell lung cancer (10 cases) – non-small cell lung cancer (480 cases); non-small cell lung cancer subdivided: cohort (3) squamous cell carcinoma (318 cases) – adenocarcinoma (194 cases) – large cell carcinoma (70 cases) was analyzed. Cohorts (1) and (2) were classified correctly in 100%, cohort (3) in more than 95%. The selected area can be limited to 10% of the original image without increased error rate. A second approach included 233 breast tissue cases (105 normal, 128 breast carcinomas) and 88 lung tissue cases (58 normal, 38 cancer). Texture analysis revealed a correct classification with only 10 training set cases in  $>92\%$  for both, breast and lung tissue. *Conclusions.* The developed system is a fast and reliable procedure to fulfill all requirements for an automated "pre-screening" of virtual slides in tissue-based diagnosis.

**Keywords:** virtual pathology, tissue-based diagnosis, automated screening, EAMUS™.

### Introduction

The technological development in computer sciences has induced new modes of medical understanding and application. For example, distributed networks transfer medical information in a standardized manner (Internet, DICOM) across continents. The digitalization of our world seems to offer numerous advantages in both the presentation of the "real" world and the display of optical (animation) environments. As a consecutive both worlds seem to melt to one complex environment. Its sources cannot be longer distinguished whether they are based on our physical data or artificially constructed information. The presentation of any information in "numbers" permits a time and space independent storage and retrieval [1–3]. In addition, context information can be achieved in future by application of new analyzing techniques unknown at the time of information acquisition.

Surgical pathology is a medical discipline intensively involved in biological and information research [4–6]. It comprises no longer the classical diagnoses in terms of tuberculosis or cancer. It includes

already statements about the probable future fate of the patient or genetic aspects [1, 7]. Therefore, the modern sentence of tissue-based diagnosis corresponds more accurate to the described pattern, as all diagnoses rely on tissue or its compartments.

The complete digitalization of histological (glass) slides is to be introduced in several routine laboratories of surgical pathology at present [8–11]. The image acquisitions machines are called slide scanners and do no longer reflect to the basic appearance of a conventional microscope. They acquire the digital presentation of the complete glass slide including the potential display of any area of the slide at any magnification within the limitations of light optics [12].

In other words, the derived virtual microscopy can visualize any tissue compartment starting from an image overview (complete glass slide) and the field of view at highest magnification ( $\times 100$  objective), which results in a resolution of  $0.5 \mu\text{m}/\text{pixel}$  [1, 12, 13]. Having these characteristics in mind, it seems appropriate to analyze potential, theoretical, and practical features in order to assist the surgical pathologist in tissue-based diagnosis. The associated main questions comprise:

- What are the image features, which contain the diagnosis-related information?
- Which or how many image compartments have to be analyzed in order to obtain a correct diagnosis?
- What are the appropriate algorithms to perform a computerized (automated) slide screening?
- Can these algorithms successfully implemented, and, if yes, what are the results in terms of diagnosis sensitivity and specificity?

These questions will be discussed in this article.

## ☞ Theoretical considerations

### Tissue-based diagnosis related image features

The information content of histological images can be distinguished into object – related and texture – related items [14–16]. Analogue to speech or text analysis the objects refer to identified and known units such as letters or words, whereas the texture refers to complex and often only crude defined image properties, called context in speech analysis. The characteristics of image information content are shown in (Table 1), those of object sizes and information extraction in (Table 2).

**Table 1 – Survey of image information compartments that contribute to tissue-based diagnosis**

Feature	Identification method	Derived parameters
Object	Segmentation, spatial analysis (measurement), stereology	Biological classification (cell type), quantitative assessment (size, surface, gray values, etc.)
Structure	Syntactic structure analysis	Orders of structure, biological units of function (vessel, bronchus, gland, etc.)
Texture	Filters, auto-regression model	Basic patterns, entropy and gray value boundary calculations

**Table 2 – Survey of frequently viewed biological objects, adequate objective, and field of view**

Search for	Objective	Field of view [mm <sup>2</sup> ]
Nucleus	×40 and higher	0.03 and lower
Cell types	×20 and higher	0.1 and lower
Small vessels, bronchioles	×10 and higher	0.55 and lower
Glands, vessels, nerves	×4–×10	3.5–0.55

The information of a digital histological, i.e. two-dimensional image is related to the plane of the image area and the gray values of the color space. The digitalization induces two separate coordinates of the plane and usually three coordinates of the color space, i.e. a five dimensional matrix [15, 17].

At least one out of the five coordinates serves for the separation of objects from the other image compartments, which are called background. The object space does not overlap with the background in each of the color dimensions. Different kinds of objects are usually identified by use of object features, such as size, color distribution, or surface.

The different kinds of objects can be correlated to each other and be analyzed in respect to potential repeating spatial associations, i.e. symmetry operations. The computed results might present with closed areas

such as rings, planes, holes, or lines, or point agglutinations, etc. These arrangements can be considered as new objects. In tissue-based diagnosis they correspond to new biological functional units such as glands, vessels, bronchi, nerves, etc. Obviously, the presence, absence, or abnormal appearance of these units is of diagnostic value too.

The described algorithm can be repeated several times, and arranged in a sequential hierarchical order [18–22]. The concept is called order of biological structures. It has been successfully applied to extracting diagnosis – relevant information from histological images [20, 23, 24].

Thus, the tissue-based diagnosis or image classification relies on objects that can be identified in an image and their spatial arrangement, which is called structure. The accurate separation of objects commonly takes place in two steps, namely: (a) separation of the object space, and (b) identification of objects from non-wanted units, for example artifacts. The procedure is called segmentation and is a prerequisite to compute or identify objects and their corresponding structures, in contrast to evaluating the image texture [12, 25–27].

The definition of a texture is not unique, and often not really useful for digital applications. According to Tamura H *et al.* an image texture is a composition of coarseness, contrast, directionality, line-likeness, regularity, and roughness [28].

This definition is not standardized, and numerous applications can be chosen which will result in quite different structure parameters of the same image. A more precise approach has been described by Voss and Süssé, and is based upon auto-regression functions derived from time series analysis [29].

Gray values of the left sided and above located pixels (4), together with an added independent random term are used to calculate the actual gray value (a total of five parameters).

The inverse application can be used to derive texture features from an image (the random expectation and the total value should become a minimum). The mathematical formulation written in matrix language is shown in (Figure 1); that of derived textures in (Figure 2).

The original image can either be analyzed using the obtained parameters, or in calculation derived parameters from the image obtained from the reverse procedure, i.e. from the image displaying the texture [29]. Useful parameters of the second application are, for example, the image entropy or specific transformation that can recognize gray value frequency distributions. These include Fourier analysis and local image filters.

### Tissue-based diagnosis related image size

Naturally, the described algorithms can be applied at different image magnifications. Texture analysis is related to the number of pixels, and mainly depends upon the size of the original image. Using an auto-correlation function, the image size should be at least 10 times multiplied by the dimensions of the recursive matrix.

**Definition**

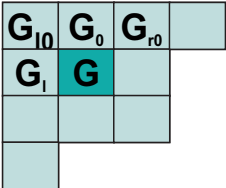
Textures can be defined by coarseness, contrast, directionality, line-likeness, regularity and roughness according to Tamura et al. (1978),

or as a n

auto-regression function derived from the analysis of time sequences (K. Voss):

$$S_i = (b_n * X_{i-n}); \quad i \{ \dots, -1, 0, +1, \dots \}$$

$S_i$  = Sequence of independent random values with expectation values  $E(S_i)=0$  and identical dispersions  $s_2$ . This can be transferred in the matrix equation:

$$\begin{pmatrix} A_{0,0} & A_{1,0} & A_{2,0} & A_{-2,1} \\ A_{1,0} & A_{0,0} & A_{1,0} & A_{-1,1} \\ A_{2,0} & A_{1,0} & A_{0,0} & A_{-2,1} \\ A_{-2,1} & A_{-1,1} & A_{-2,1} & A_{0,0} \end{pmatrix} * \begin{pmatrix} a_{1,0} \\ a_0 \\ a_{r0} \\ a_1 \end{pmatrix} = \begin{pmatrix} A_{1,1} \\ A_{1,0} \\ A_{-1,1} \\ A_{1,0} \end{pmatrix}$$


Using  $S = E( [a_{10}G_{x-1,y-1} + a_0G_{xy-1} + a_{x0}G_{x+1,y-1} + a_1G_{x-1,y} + R_{x,y} - G_{x,y}]^2 ) \rightarrow \text{minimum}$   
 A six dimensional stochastic differential equation describes the correlation of random values (gray values)

Figure 1 – Mathematical formulation of the applied auto-regression algorithm to reproducibly analyze image textures (according to [43])

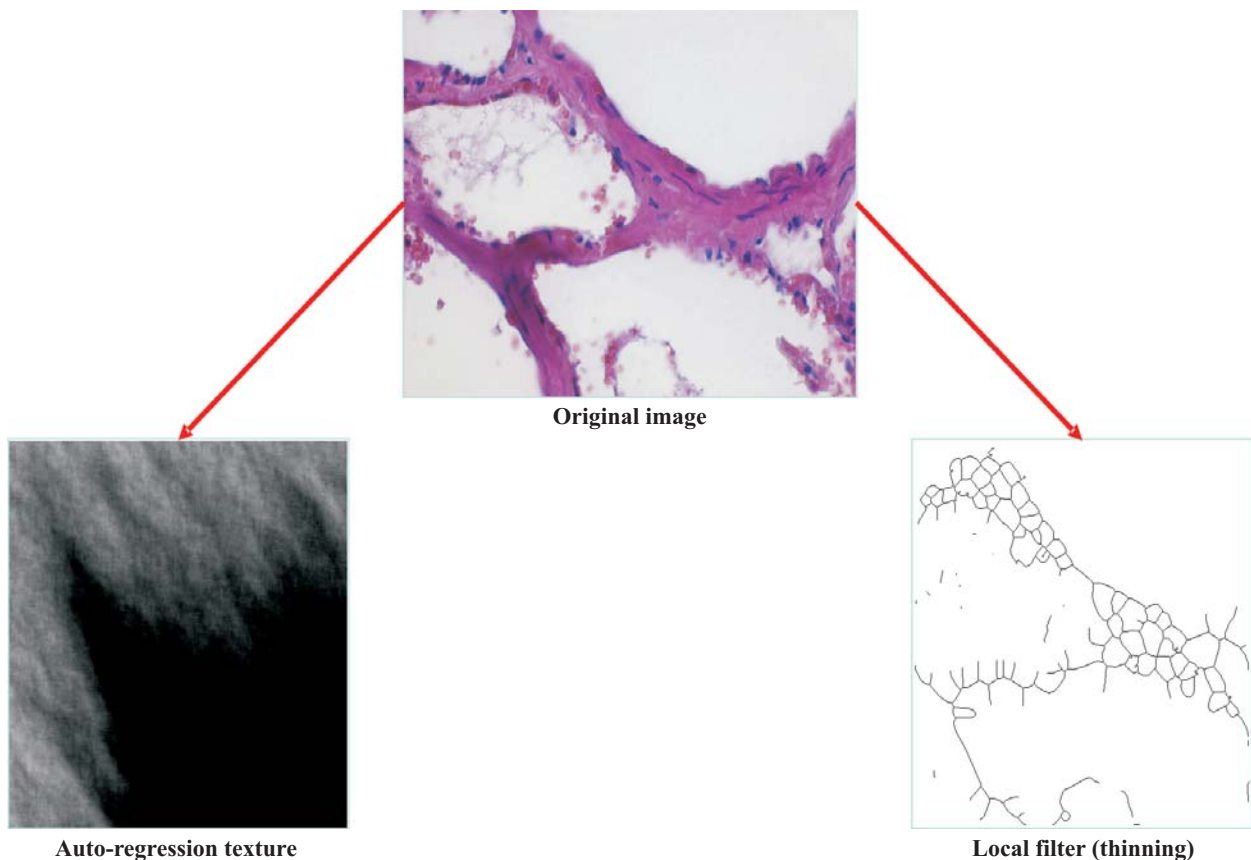


Figure 2 – Derived textures of a histological image (normal lung; HE staining,  $\times 40$ )

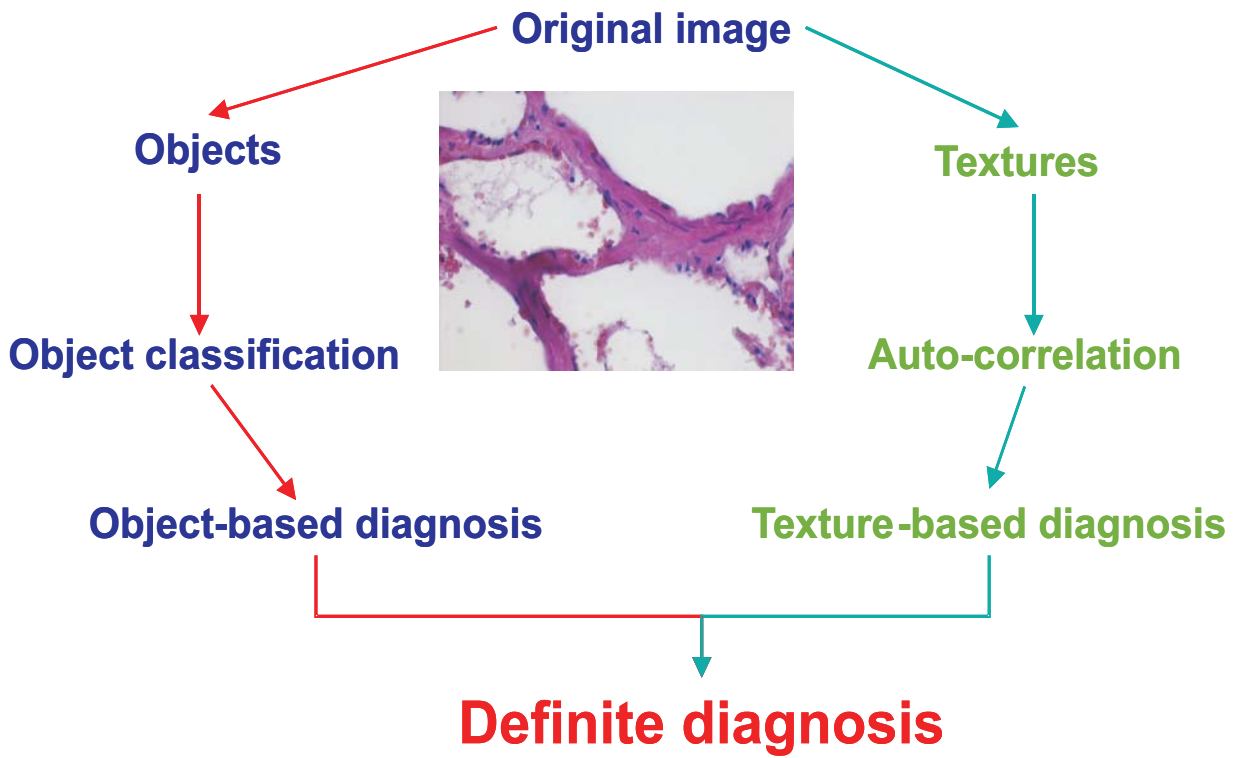


Figure 3 – Scheme of object and texture related feature extraction to computing tissue-based diagnoses

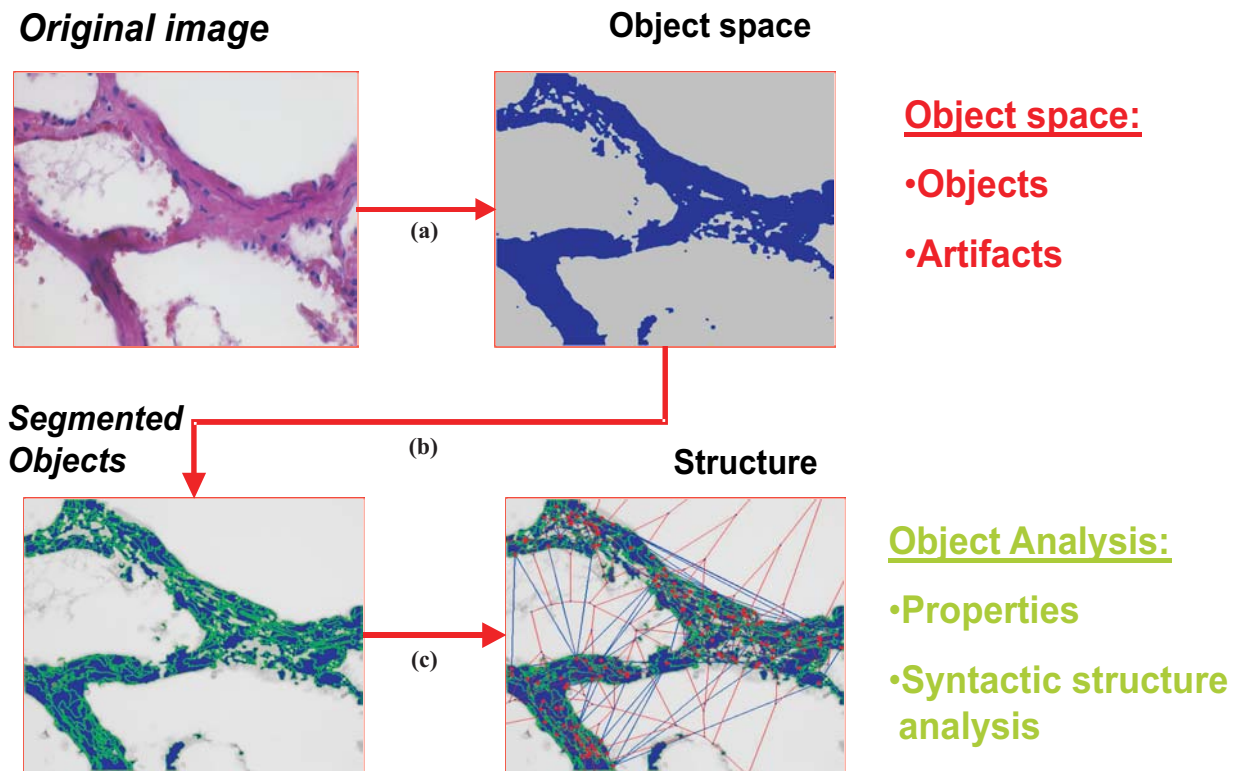


Figure 4 – The algorithm to analyzing object associated image information includes: (a) a separation of the image into object space and background, (b) object segmentation and identification within the object space, and (c) syntactic structure analysis to identifying spatial relationships between identified objects

Having a matrix  $5 \times 3$ , the smallest image size should be  $50 \times 30$  pixels. The differentiation between different textures requires again about 10 times larger images, and the specificity remains quite low if smaller images are subject for texture analysis based upon recursive algorithms [1].

Object identification, again, depends upon the number of object pixels, which are the basis for correct identification. Object sizes of 50 pixels are probably the absolute minimum to allow correct object identification. For practical purposes, object sizes should comprise about 300–500 pixels. To accurately state an object-related diagnosis depends upon the accuracy of object identification. For example, the diagnosis "cancer" can be definitely stated if only one individual "cancer cell" can be identified with absolute certainty. This theoretical certainty does not or only rarely exists in routine tissue-based diagnosis, and a minimum number of 10–20 diagnosis – related objects should be a prerequisite for a diagnosis statement in cytology [1]. This number can be decreased to 1–2 events in higher order structures, such as caseating granulomas characteristic for tuberculosis or inflammatory vascular infiltrations characteristic for vasculitis. Thus, a minimum number of at least 50–100 objects should be identified in the field of view of automated virtual microscopy to assure a correct object identification and related diagnosis. The minimum size of the field of view can then be calculated to 40 000 pixels or a dimension of  $200 \times 200$  pixels (50 objects of 400 pixels, two times over-sampling).

The identification of nuclei is the most frequently applied segmentation method in tissue-based diagnosis. The average nuclear size amount to 10–15  $\mu\text{m}$  in diameter, and can be accurately defined using an objective  $\times 20$ – $\times 40$ . The obtained nuclear pixel size measures 100–300 pixels and usually 100–500 nuclei can be identified in the field of view to our experience. The preferred magnification to be applied in automated tissue-based diagnosis should be, therefore, related to an objective  $\times 20$ .

### Tissue-based diagnosis related algorithms

The derived algorithm to be applied in automated tissue-based diagnosis should include both texture – and object – related information acquisition techniques. The general scheme proposed by Kayser K *et al.* [11] is shown in (Figure 3). The original image is subject to a texture analysis contemporary to a segmentation procedure to detect potential objects. The texture analysis can be performed on the original image or on images that have undergone various transformations, such as thinning, Hough, Prewitt, Fourier, or Hadamard operations. The calculated image entropy or the auto-recursive parameters serve for image description and are subject to discriminate between diagnosis classifications. No external information is required to analyze image textures.

Image segmentation and object identification require some external information to correctly identify the objects searched for. Preset upper and lower limits of object size and surface are a necessity to distinguish

objects from artifacts. The preset information can be quite crude and automatically adjusted to the correctly identified objects. Without any preset limitations biological meaningful objects cannot be automatically extracted from a histological image to our and others' experience [1, 7, 12].

A minimum percentage of 90–95% of all objects within a field of view can be segmented using dynamic thresholding and external knowledge [1, 7, 12]. This percentage permits a correct structure analysis which commonly only includes relations between identical objects, or two different object classes. A characteristic example is given in (Figure 4).

An appropriate analysis of spatial relationships is the so-called syntactic structure analysis, a technique that is based upon graph theory and a predefined neighborhood algorithm [17, 30].

Voronoi's and the complementary Delaunay's tessellation are the most frequently applied methods [31, 32]; O'Callaghan's neighborhood condition is useful too [33, 34]. Derived parameters include distances between nearest neighboring objects, number of neighbors, number of limited paths, etc. [23, 35]. These parameters serve for diagnosis purposes too.

Virtual slides comprise images of several GB in size, and include about 500 million pixels. It is not economic to transfer and analyze such big images at a whole. It seems more appropriate to select either by random or stratified certain areas, and deduce the obtained information in order to state a diagnosis. This procedure is permitted as the total of visual information can be formulated:

$$It = \sum \{Pv \times I(Pv)\}, \text{ with}$$

*It* – total of visual information; *Pv* – area/volume fraction of analyzed fields of view; *I(Pv)* – information content of analyzed field of view [23, 35].

The application of Nyquist's theorem can be applied to the above stated formula and allows, to calculating the minimum percentage of analyzed image areas in relation to an acceptable error rate [1]. We have to take into account that the information content of the whole image could not be larger than the information of an image partition that already permits a correct diagnosis, and Nyquist's theorem has to be adjusted adequately. In other words, the minimum number of objects, structures and textures which fully determinate a diagnosis is the critical factor in analyzing diagnosis reliable compartments of a virtual slide. The analysis of the complete slide will neither alter the diagnosis nor increase its reliability.

### Experimental approach

The following experimental approach was initiated to investigate in automated tissue-based diagnosis:

Hematoxylin–Eosin stained slides were acquired using a digital camera (Leica,  $\times 20$ ) mounted on a microscope Leica MB at the following objectives ( $\times 2$ ,  $\times 4.5$ ,  $\times 10$ ,  $\times 20$ ,  $\times 40$ ). The maximum image size measured  $1024 \times 768$  pixels. Self-written programs based upon DIAS (DIAS, University Jena, Germany) analyzed the textures, object features, and object related structure

at various image sizes (128×128, 256×256, and 512×512 pixels).

The data were fed into a classification program to automatically classify the images separately for each image size.

In study (1) a total of 808 lung tissue cases (318 normal tissue cases, 216 epidermoid carcinoma cases, 194 adenocarcinoma cases, 70 large cell carcinoma cases, and 10 small cell lung cancer cases) have been analyzed.

In study (2) a total of 128 additional breast and 30 lung cancer cases, as well as 105 normal breast and 58 normal lung tissues was subject for classification by texture analysis.

A teaching set comprising 10 cases of normal breast and lung tissue and of breast and lung cancer each served for training the classifier.

## ☐ Results

The results of the prescreening between normal tissue – cancer tissue of study (1) are presented in (Figure 5), that of the study (2) in (Figure 6).

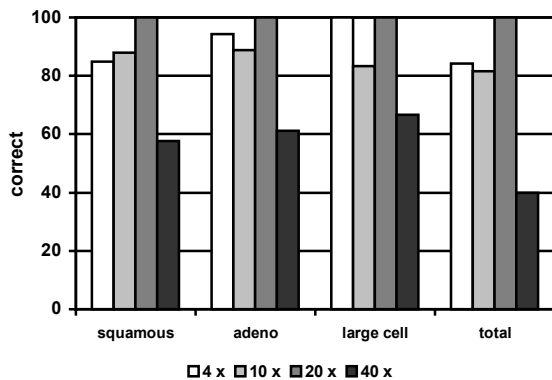


**Figure 5 – Classification results of study (1) comprising 808 lung tissue cases (318 cases with normal lung, 216 cases with epidermoid carcinoma, 194 cases with adenocarcinoma, 70 cases with large cell anaplastic carcinoma, 10 cases with small cell lung cancer): all tumor entities have been correctly classified using an objective ×20**

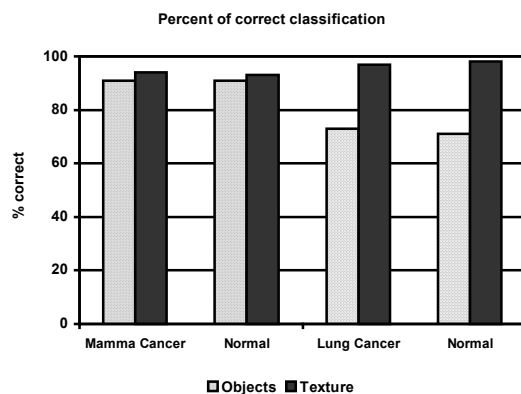


**Figure 6 – Classification results of study (2): a 92–98% percentage of correct classification based upon texture analysis only was obtained in both breast and lung cancer cases. A training set of 10 cases each only is sufficient to correctly classify all case with an accuracy >92%**

The individual correct classification ranged between 92–98% using the texture approach, and between 70–95% using the object approach. The highest accuracy was obtained in fields of view acquired with an objective ×20. The specificity and sensitivity of classification dropped for image sizes of 128×128, and remained the same for images >256. In general, the results confirm the theoretical considerations that image sizes of at least 256×256 pixels are necessary to reliably extract visual information from histological slides for tissue-based diagnosis.

## ☐ Discussion

Automated screening in tissue-based diagnosis goes back into the early 1990s when the first approaches of successful computerized cytology screening have been reported [36].

The shortage of cytology assistants in the U.S.A. forced the development of these systems, which have been approved by the Federal Drug Administration (FDA) and introduced into routine work by some cytology institutions. Successful cytology screening depends upon the quality of the smears to a great extent, and specific methods to separate in display individual cells are mandatory for automated screening application in general [36].

The diagnosis information of cytology is only object related at the order of individual cells or nuclei, and texture associated information does not play a role in contrast to visual information of light microscopy tissues. The first approaches to associate visual information of histological slides with the diagnosis were related to object features, and subject to intensive research in stereology [37–40].

The analysis of structures and textures ranges back to the early 1980s when Kayser K *et al.* and Sanfeliu A *et al.* reported the first successful analysis of histological textures in association with the underlying diagnosis [24, 41]. These early approaches were still interactive. Contemporary with the development in computer technology new approaches were reported, and Bartels P *et al.* applied the ideas to discriminate between prostate carcinomas and their pre-neoplastic lesions [42–44].

A similar and unique approach has been reported from Leong FJ, who could derive quite detailed diagnoses from breast carcinoma slides automatically [12]. All these new investigations are closely related to Telepathology, and it is not by accident that pioneers in Telepathology are involved in digital pathology too [3, 45].

Digital or virtual pathology is based upon the digitalization of a complete glass slide [1]. Commercially available glass slide scanners can acquire the images of about 200–400 glass slides per day/night and are to be introduced into routine tissue based diagnosis in the near future [8].

Pathologists can view a virtual slide in the conventional manner. It offers, in addition, the chance to be automatically analyzed prior to the pathologist's view.

## ☐ Conclusions

Our theoretical considerations and practical investigations clearly demonstrate that:

- automated screening of virtual slides is possible with high accuracy, at least in breast and lung cancer.
- they can be performed with high accuracy.
- they do not necessarily require segmentation procedures.
- they can be applied for images or image compartments of quite low size (512×512) pixels without diminished accuracy.

The results are in agreement with data reported from Telepathology and from previous studies in terms of specificity and sensitivity. The procedures can be combined with automated immunohistochemical measurements, which are now available in the Internet (EAMUS™; www.eamus.de), and open a new door into the world of understanding and extraction visual information for tissue-based diagnosis.

## Acknowledgements

The financial support of the International Academy of Telepathology and the *Verein zur Förderung des Biologisch-Technologischen Fortschritts in der Medizin* is gratefully acknowledged.

## References

- [1] KAYSER K., KAYSER G., Virtual microscopy and automated diagnosis. In: GU J., OGILVIE R. (eds), *Virtual microscopy and virtual slides in teaching, diagnosis and research*, Taylor & Francis, Boca Raton, 2005.
- [2] KAYSER K., KAYSER G., RADZISZOWSKI D., OEHMANN A., *New developments in digital pathology: from telepathology to virtual pathology laboratory*, Stud Health Technol Inform, 2004, 105:61–69.
- [3] KAYSER, K., SZYMAS J., WEINSTEIN R. S., *Telepathology and telemedicine communication, electronic education and publication in e-health*, Veterinärspiegel Verlag, Berlin, 2005.
- [4] LEE E., CHAE Y., KIM I. et al., *Prognostic relevance of immunohistochemically detected lymph node micrometastasis in patients with gastric carcinoma*, Cancer, 2002, 94(11):2867–2873.
- [5] LEONG, A.S. AND F.J. LEONG, *What we need to know about cancer genes*. Diagn Cytopathol, 1998, 18(1): p. 33–40.
- [6] LEONG, A.S., et al., *An advanced digital image-capture computer system for gross specimens: a substitute for gross description*. Pathology, 2000, 32(2): p. 131–5.
- [7] KAYSER G., RADZISZOWSKI D., BZDYL P. et al., *Theory and implementation of an electronic, automated measurement system for images obtained from immunohistochemically stained slides*, Anal Quant Cytol Histol, 2006, 28(1):27–38.
- [8] MOLNAR B., BERCZI L., DICZHAZY C. et al., *Digital slide and virtual microscopy based routine and telepathology evaluation of routine gastrointestinal biopsy specimens*, J Clin Pathol, 2003, 56(6):433–438.
- [9] OKADA D.H., BINDER S.W., FELTEN C.L. et al., *"Virtual microscopy" and the internet as telepathology consultation tools: diagnostic accuracy in evaluating melanocytic skin lesions*, Am J Dermatopathol, 1999, 21(6):525–531.
- [10] WEINSTEIN R. S., *Innovations in medical imaging and virtual microscopy*, Hum Pathol, 2005, 36(4):317–319.
- [11] WEINSTEIN R. S., DESCOUR M. R., LIANG C. et al., *An array microscope for ultrarapid virtual slide processing and telepathology. Design, fabrication, and validation study*, Hum Pathol, 2004, 35(11):1303–1314.
- [12] LEONG F. J., *An automated diagnostic system for tubular carcinoma of the breast – a model for computer-based cancer diagnosis*, Department of Engineering Science, DPhil Thesis, Oxford University, 2002, 250.
- [13] LEONG F. J., LEONG A. S., *Digital imaging applications in anatomic pathology*, Adv Anat Pathol, 2003, 10(2):88–95.
- [14] KAYSER K., KIEFER B., BURKHARDT H. U., *Syntactic structure analysis of bronchus carcinomas – first results*, Acta Stereol, 1985 4(2):249–253.
- [15] KAYSER K., SZYMAS J., WEINSTEIN R. S., *Telepathology: telecommunication, electronic education and publication in pathology*, Springer Verlag, Berlin–Heidelberg–New York, 1999.
- [16] KAYSER K. K., MODLINGER F., POSTL K., *Quantitative low-resolution analysis of colon mucosa*, Anal Quant Cytol Histol, 1985, 7(3):205–212.
- [17] KAYSER K., HUFNAGL P., KAYSER G., ZINK S., *Stratified sampling: basic ideas and application in pathology*, Elec J Pathol Histol, 1999, 5:994–1006.
- [18] KAYSER K., BERTHOLD S., EICHORN S. et al., *Application of attributed graphs in diagnostic pathology*, Anal Quant Cytol Histol, 1996, 18(4):286–292.
- [19] KAYSER K., GABIUS H. J., *Graph theory and the entropy concept in histochemistry. Theoretical considerations, application in histopathology and the combination with receptor-specific approaches*, Prog Histochem Cytochem, 1997, 32(2):1–106.
- [20] KAYSER K., HAGEMEYER O., *Stage related morphometry of sarcoid granulomas and inflammatory cell types in broncho-alveolar lavage*, Anal Cell Pathol, 1991, 3(6):335–342.
- [21] KAYSER K., STUTE H., BUBENZER J., PAUL J., *Combined morphometrical and syntactic structure analysis as tools for histomorphological insight into human lung carcinoma growth*, Anal Cell Pathol, 1990, 2(3):167–178.
- [22] KAYSER K., STUTE H., TACKE M., *Minimum spanning tree, integrated optical density and lymph node metastasis in bronchial carcinoma*, Anal Cell Pathol, 1993, 5(4):225–234.
- [23] KAYSER K., KAYSER G., HUFNAGL P., *The concept of structural entropy: basic idea and applications*, Elec J Pathol Histol, 2002, 8:24–26.
- [24] KAYSER K., SCHLEGEL W., *Pattern recognition in histopathology: basic considerations*, Methods Inf Med, 1982, 21(1):15–22.
- [25] KAYSER G., BAUMHAKEL J. D., SZOKE T. et al., *Vascular diffusion density and survival of patients with primary lung carcinomas*, Virchows Arch, 2003, 442(5):462–467.
- [26] KAYSER K., et al., *New developments in digital pathology: From telepathology to virtual pathology*. In: DUPLAGA M., ZIELINSKI K., INGRAM D. (eds), *Transformation of health care with information technologies*, IOS Press, Amsterdam, 2004, 61–69.
- [27] LUNDIN M., LUNDIN J., HELIN H., ISOLA J., *A digital atlas of breast histopathology: an application of web based virtual microscopy*, J Clin Pathol, 2004, 57(12):1288–1291.
- [28] TAMURA H., MORE S., YAMAWAKI T., *Texture features corresponding to visual perception*, IEEE Trans, Systems Man and Cybernetics (SMC), 1978, 8:460–473.
- [29] VOSS K., SÜBE H., *Praktische Bildverarbeitung*, Carl Hauser Verlag, München–Wien, 1991.
- [30] KAYSER G., RIEDE U., WERNER M. et al., *Towards an automated morphological classification of histological images of common lung carcinomas*, Elec J Pathol Histol, 2002, 8:22–30.
- [31] VAN DIEST P. J., KAYSER K., MEIJER G. A., BAAK J. P., *Syntactic structure analysis*, Pathologica, 1995, 87(3):255–262.
- [32] VORONOI G., *Nouvelles applications des paramètres continus à la théorie des formes quadratiques, deuxième mémoire: recherches sur les paralléloèdres primitifs*, J Reine Angew Math, 1902, 134:188–287.
- [33] KAYSER K., Application of structural pattern recognition in histopathology. In: FERRATÉ G., SANFELIU A., BUNKE H. (eds), *Syntactic and structural pattern recognition*, Springer Verlag, Berlin–Heidelberg–New York, 1988, 115–135.
- [34] O'CALLAGHAN J. F., *An alternative definition for neighborhood of a point*, IEEE Trans, Comput, 1975, 24:1121–1125.
- [35] KAYSER K., GABIUS H. J., *The application of thermodynamic principles to histochemical and morphometric tissue research: principles and practical outline with focus on the glycosciences*, Cell Tissue Res, 1999, 296(3):443–455.

- [36] HUSAIN O. A., WATTS K. C., LORRIMAN F. *et al.*, *Semi-automated cervical smear pre-screening systems: an evaluation of the Cytoscan-110*, *Anal Cell Pathol*, 1993, 5(1):49–68.
- [37] BARTSCH G., FRICK J., ROHR H. P., *Stereology, a new morphological method of study prostatic function and disease*, *Prog Clin Biol Res*, 1976, 6:123–141.
- [38] CRUZ-ORIVE L. M., WEIBEL E. R., *Recent stereological methods for cell biology: a brief survey*, *Am J Physiol*, 1990, 258(4 Pt 1):L148–156.
- [39] ELIAS H., BOKELMANN D., VOGTLE R., *Principles of stereology and morphometry presented with large intestinal carcinogenesis as example*, *Verh Anat Ges*, 1976, 70(Pt 2):911–916.
- [40] GUNDERSEN H. J., *Stereology or how figures for spatial shape and content are obtained by observation of structures in sections*, *Microsc Acta*, 1980, 83(5):409–426.
- [41] SANFELIU A., FU K. S., PREWITT J., *An application of distance measure between graphs to the analysis of muscle tissue pattern recognition*, *Proceedings of the Saratoga Springs Meeting*, New York, 1981, 86–89.
- [42] BARTELS P. H., WEBER J. E., DUCKSTEIN L., *Machine learning in quantitative histopathology*, *Anal Quant Cytol Histol*, 1988, 10:299–306.
- [43] BARTELS P. H., *Computer-generated diagnosis and image analysis. An overview*, *Cancer*, 1992, 69(6 Suppl):1636–1638.
- [44] BARTELS P. H., BARTELS H. G., MONTIRONI R. *et al.*, *Machine vision in the detection of prostate lesions in histologic sections*, *Anal Quant Cytol Histol*, 1998, 20(5):358–364.
- [45] KAYSER G., KAYSER K., *Telepathology in Europe*. In: Gu J. (ed), *Virtual microscopy and virtual slides in teaching, diagnosis and research*, Taylor & Francis, Boca Raton, 2005.

### **Mailing address**

Klaus Kayser, M. D., Ph. D., Director UICC–TPCC, Institute of Pathology, Charité, University of Berlin, 20/21 Schumann Street, D–10117 Berlin, Germany; E-mail: klaus.kayser@charite.de

*Received: July 6<sup>th</sup>, 2006*

*Accepted: July 20<sup>th</sup>, 2006*